Deciphering the structure of tungstate and molybdate complexes with glucose, mannose and erythrose

Sabah El Mohammad,[a] Sandrine Develle,[a] Olivier Proux,[b] Antonio Aguilar,[c] Jean-Louis Hazemann,[d] Christèle Legens,[a] Céline Chizallet[a] and Kim Larmier[a]*

a IFP Energies nouvelles, Rond-Point de l'Echangeur de Solaize, 69360 Solaize, France.

b OSUG, UAR 832 CNRS, Université Grenoble Alpes, 38041, Grenoble, France

c ICMG, UAR 2607 CNRS, Université Grenoble Alpes, 38041, Grenoble, France

d Institut Néel, CNRS, Université Grenoble Alpes, 25 Avenue des Martyrs, 38042, Grenoble, France

ABSTRACT Combining NMR, XANES and DFT, we elucidate the structures of tungstate and molybdate with sugars of interest in the conversion of biomass to platform chemicals (glucose, mannose and erythrose). We highlight a number of complexes, including one nearly isostructural structure that is formed with each metal-sugar combination. We also emphasize the singular reactivity of erythrose, that undergo retro-aldolisation at room temperature.

KEYWORDS Biomass, Carbohydrate, DFT, NMR, XAS, Tungstates, Molybdates

Introduction

The transformation of biomass-based carbohydrates into platform chemicals is a topical issue for the replacement of petroleum-based resources in the chemical industry.[1] Ethylene glycol (EG) is one of the main targets for the development of such a process, with a world production of around 20 Mty.[2] The direct synthesis of ethylene glycol from sugars (mainly glucose) relies on the sequence of two main reactions: the retro-aldolization of glucose into a key intermediate, glycolaldehyde, and the hydrogenation of this molecule into EG.[3] The first reaction is the most challenging of the two as it needs to be very selective with respect to other reactions (isomerization, degradation reactions etc.). In last decades, homogeneous catalysts based on tungsten or molybdate (to a lesser extent) oxyanions in aqueous solutions have proven quite effective, affording yields as high as 70-80 % from glucose when used in combination with a hydrogenation catalyst (such as Ni/C or Ru/C).[4–8] However, the reasons explaining the particularity of such catalysts remain to date unclear on a molecular point of view. At the origin of the chemical reactivity, tungstate or molybdate ions need to interact with the sugar, forming complexes in solution.[9–13] Understanding the nature of the species formed, and the conditions in which they exist, is a prerequisite for understanding the reactivity of such systems. In a recent contribution, we proposed a methodology using a combination of spectroscopies (Nuclear Magnetic Resonance NMR, X-Ray Absorption Spectroscopy Near Edge Structure XANES) and molecular modelling at the Density Functional Theory level (DFT) to study the speciation of complexes of mannose and tungstate ions as a prototypical case and proposed molecular models for each species observed.[14] Herein, we apply this same methodology to extend the scope of the study and include other sugars involved in the conversion of biomass-based sugars (glucose and erythrose) into EG over both sodium tungstate and sodium molybdate in aqueous solution.

Methods

All chemicals are purchased from Sigma-Aldrich and used as received. Each data point consists of an independent sample, prepared according to the following method: the desired amounts of metallic precursor and sugar are dissolved in water, then the pH is adjusted to the desired value by addition of a few drops of aqueous HCl (37 %wt) or NaOH (15 %wt). The pH value is controlled using a standard pH-meter. Unless otherwise stated, the NMR spectra are taken within two hours after the preparation of the samples. In some experiments Dimethylsulfoxide (DMSO) was mixed with D_2O (0.5 M) and serves as an internal standard for referencing and quantification purposes (δ (^{1}H) = 2.5 ppm, δ (^{13}C) = 39.5 ppm). NMR spectra were recorded on a Bruker Advance III spectrometer (300 MHz) at 300 K. When performed, the quantification are done by integration of the signal of the anomeric carbon relative to that of the free sugar. XANES spectra were acquired in transmission mode at the European Synchrotron Radiation Facility (Grenoble, France) at the CRG-FAME BM30 beamline.[15,16] Energy calibration was ensured by measuring the XAS signal of a W or Mo metallic foil in double transmission, with reference energies set at 10207 eV and 20000 eV respectively. DFT calculations were performed using the Gaussian09 software suite,[17] using the B3LYP exchange-correlation functional,[18–20] a TZVP basis set for C, H and O atoms and def2-TZVP for Mo and W atoms.[21–23] Chemical shielding are calculated using the Gauge-Independent Atomic Orbitals (GIAO) method as implemented in Gaussian, and chemical shifts are calculated with respect to calculated DMSO. The energetic data is provided in supporting information along with the full calculation methodology. Additional detail is provided in the supporting information.

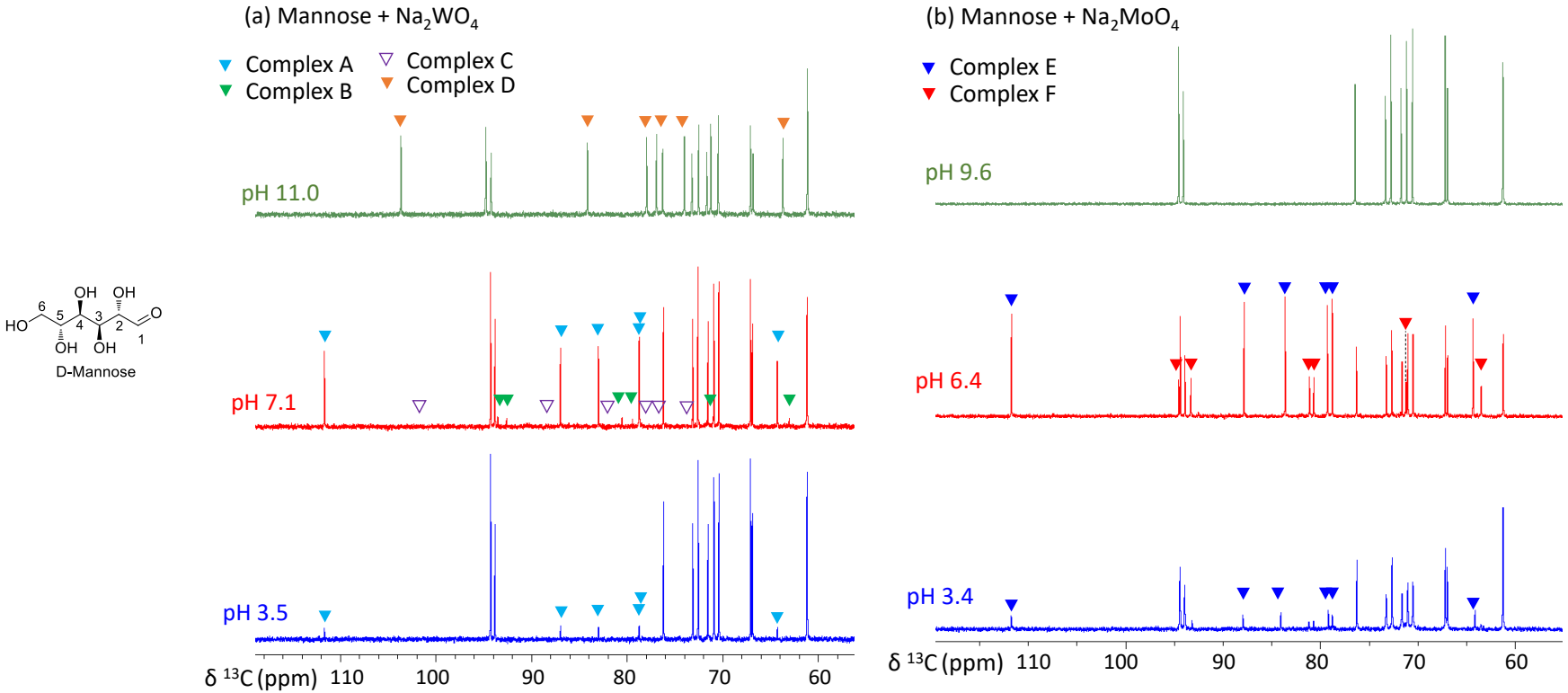

Figure 1. Proton decoupled ^{13}C NMR spectrum of mannose aqueous solution with (a) tungstate (b) molybdate ions at different pH ranges. [M] = 2 mol L^{-1}, [sugar] = 1 mol L^{-1}. Unlabelled peaks in each figure correspond to the free sugar remaining in the solution. Spectra are recorded 1 hour after preparation. Note that though the signals assigned to Complex C are not clearly visible on this picture, they are identified on the 2D spectra reported on Figure S1-S2.[14] All spectra are scaled and referenced to the peak of DMSO (at 39.5 ppm, not shown) added in D_2O at a concentration of 0.5 M. Total concentration of sugars and complex determined through internal standard technique is in each case of 1.0 ± 0.1 mol L^{-1}. For the evolutions over 240 h see Figure S4-S5 in Supporting Information.

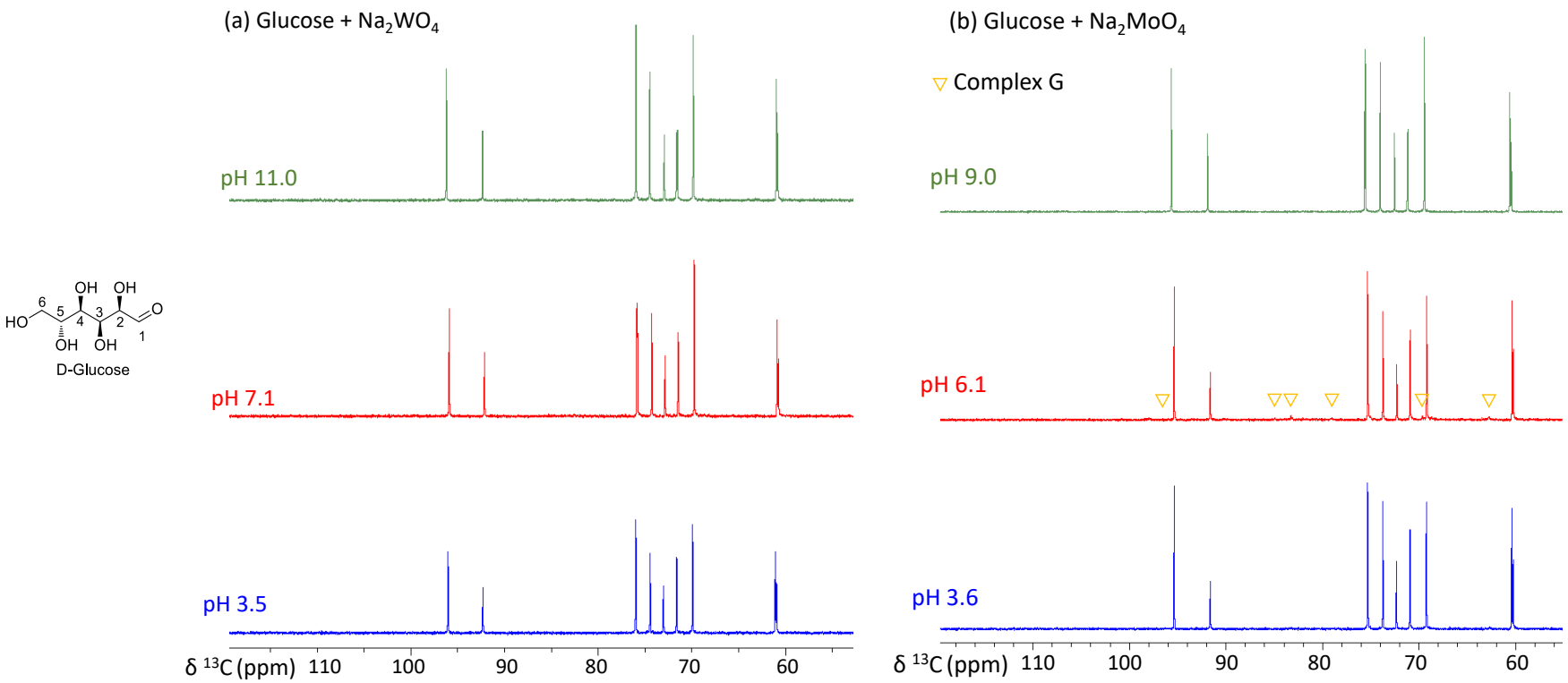

Figure 2. Proton decoupled ^{13}C NMR spectrum of glucose aqueous solution with (a) tungstate (b) molybdate ions at different pH ranges. [M] = 2 mol L^{-1}, [sugar] = 1 mol L^{-1}. Unlabelled peaks in each figure correspond to the free sugar remaining in the solution. Spectra are recorded 1 hour after preparation. Note that though the signals assigned to Complex G are not clearly visible on this picture, they are identified on the 2D spectra reported on Figure S8. For the evolution after 5 days of the Na_2WO_4 solution at pH 6, see Figure S9.

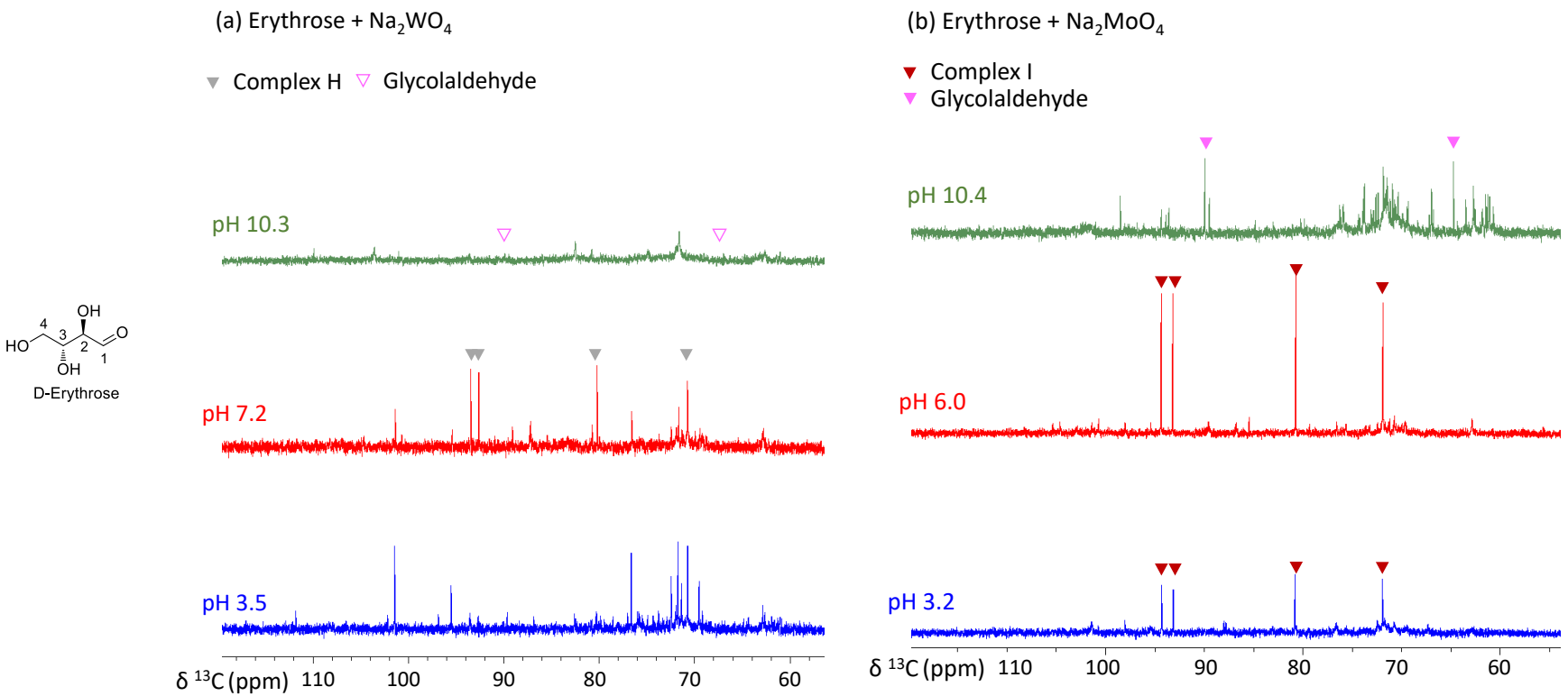

Figure 3. Proton decoupled ^{13}C NMR spectrum of erythrose aqueous solution with (a) tungstate (b) molybdate ions at different pH ranges. [M] = 2 mol L^{-1}, [sugar] = 1 mol L^{-1}. Unlabelled peaks in each figure correspond to the free sugar remaining in the solution. In the case of erythrose mixed with the metals in basic solutions, some of these peaks might be attributed to side products (such as humins). Spectra are recorded 1 hour after preparation. Note that the presence of glycolaldehyde is attested by additional ^{1}H and correlation spectra presented in Figure S10-S13 in the case of Mo mixtures and only suggested by analogy in the case of W mixtures. For the evolutions over time see Figure S14.

Results and Discussion

Figures 1-3 show the ^{13}C NMR spectra of aqueous solutions of each sugar under study (mannose, glucose or erythrose) with either sodium tungstate or sodium molybdate. Metal and sugars are introduced in a molar ratio of 2, and we adjust the pH value by addition of small quantities of either HCl or NaOH solutions (see 2D spectra in Figures S1-S2). Figure 1a reproduces the behavior of W-mannose solutions as described in our previous study.[14] In short, three new species **A**, **B** and **C** appear in the acidic-to-neutral pH range, with a maximum in concentration at pH = 7.1, while a fourth species **D** exists exclusively in basic pH (above 9). In the presence of molybdate instead of tungstate, mannose forms only two complexes (Figure 1b), labelled Complex **E** (major species) and Complex **F** (minor species). Both are at most abundant in neutral solution, exist at acidic pH although in much lower abundance, and are absent in basic solutions, where no complex is observed, contrary to their behavior with tungstate (see Figure S3 reporting concentration vs. pH of these complexes). The concentration of both species reaches a maximum at pH around 6.5, at which the total amount of complexed sugar is of 58 %. Considering the metal-to-sugar ratio, the maximum nuclearity of these complexes should be of at most 3.4. Akin to the case of tungstate ions, note that similar results are obtained when using ammonium heptamolybdate (AHM) provided that the pH value is similar, thus the pH is the most determining parameter in the speciation. We evaluated the stability of these species by monitoring the evolution of the spectra over time (up to 240 h) with respect to an internal standard (DMSO, see Figures S4-S5). In most cases, the mixtures are quite stable over two weeks, and the different species do not interconvert or form other species. In two cases, however, namely mannose + Na_2MoO_4 pH 3.5 and mannose + Na_2WO_4 pH 10, we see a significant decrease in the intensity of the signals, relative to the standard DMSO. No significant other species are observed, so that we assign this to decomposition of the sugar into unidentified

degradation products, such as humins. However, the rate of the decrease is quite slow, and after 24 h less than 20 % of the signals have disappeared. We may then conclude the mannose solutions are at equilibrium in the time frame at which the spectra were recorded (within the first couple of hours after their preparation).

In the case of glucose (Figure 2), we observe no evidence for the formation of new species with tungstate, regardless of the pH of the solution (Figure 2a). Spectra recorded at pH 7 using 1-^{13}C glucose and 3-^{13}C glucose (Figures S6 and S7) show two sets of peaks, showing that at least two species are formed in this pH range, labelled complexes **P1** and **P2**, albeit their abundance is extremely low (below detection limit with unlabelled glucose). With molybdate, glucose affords one new species in neutral solutions (pH 6.1), (in a small amount) designated as complex **G** (Figure 2b – see also Figure S8 for assignment through 2D spectra). In the case of glucose again, the solutions are quite stable over time (see for instance Figure S9, where only minor amount of an undetermined additional species is formed in the case of glucose-tungstate at pH 7 after 5 days).

The case of erythrose is significantly more complex (Figure 3, see also 2D spectra in Figures S10-S13). Unlike the cases of glucose and mannose, the solutions tend to be quite unstable with time, and degradation is observed in most cases (except for erythrose-molybdate at pH 6.0, in which case the solution is somewhat stable – see Figure S14). We nevertheless attempted to provide a molecular description of the few species we could detect, which is still a relevant information regarding the reactivity, though maybe not sufficient. One complex is formed with molybdate and one with tungstate (labelled complex **H** and complex **I** with tungstate and molybdate respectively), existing in neutral and acidic solutions (the former is more abundant, similarly to complexes **A**, **B**, **E**, **F** and **G** with glucose and mannose). Note that complex **I** is the

only species observed in neutral solutions, with no free sugar left, which indicates the large stability of this complex. Additionally, considering that the metal-to-sugar ratio is of 2, this clearly indicates that the nuclearity of this complex is either 2 or 1. In basic solutions, though, a clearly distinct behavior occurs. With both metals, we observed a significant loss of the overall NMR signal accompanied by the appearance of a large series of low intensity signals within a couple of hours after the preparation. Among these signals, we identified traces of glycolaldehyde (by comparison with a standard), which is the product of erythrose retro-aldol condensation by cleaving the C-C bond of erythrose (see Figure S13).

This observation is singular to the case of erythrose since no such behavior was observed with mannose nor glucose although their retro-aldolisation should also yield glycolaldehyde. this reveals that erythrose is reactive at ambient temperature with tungstate and molybdate to form cleavage products, that may then lead to the formation of degradation products, hence the loss of the intensity of the NMR signal. We verified that the presence of glycolaldehyde is due to the catalysis of metals and not to the hydroxide ions present in basic solution by showing that no traces of glycolaldehyde are found when the sugar was mixed only with sodium hydroxide in the same pH range (Figure S15 in the Supporting Information). The presence of a complex under such conditions cannot be unambiguously attested by observation of the NMR signals, although it is a prerequisite for the retro-aldolisation reaction.

^{95}Mo NMR spectra of the molybdate-sugars aqueous solutions have been recorded to get additional information on the complexes formed. **Figure 4** shows the data obtained at a pH of about 6 for each sugar under study, compared to that of ammonium heptamolybdate at a similar pH. This latter species entails mostly octahedral polymolybdate species according to the speciation diagram of molybdate species in aqueous solutions (see Figure S16-S17 – mainly

$HMo_7O_{24}^{5-}$ ions). Our spectrum indeed shows a main, broad signal at 38.5 ppm, characteristic of such species with molybdenum in a octahedral geometry.[24] A residual signal at 0 ppm accounts for the coexistence of a fraction of tetrahedral MoO_4^{2-} ions in this pH range at equilibrium. The glucose-molybdate solution shows qualitatively the same signals, which is consistent with the fact that no complex is observed by ^{13}C NMR, and the molybdate speciation is not perturbed to a significant extent by the presence of glucose. On the opposite, with erythrose and mannose, the signal assigned to octahedral species is strongly perturbed, with the appearance of signals at 33.1 and 27.1 ppm in the case of erythrose, and 42.8 and 30.9 ppm in the case of mannose. This is again consistent with the formation of complexes in these mixtures. Besides, the very different signals obtained for erythrose and mannose suggests structurally different complexes. We report in Figure S18 the evolution of the mannose-molybdate and glucose molybdate signals with pH. In the case of glucose, where no complex is formed, it follows the aqueous-phase speciation of molybdate, with monomeric, tetrahedral species dominant at pH > 6 (sharp peak at 0 ppm) and a broad signal at 38.5 ppm dominant at pH between 4 and 6. In the case of mannose, the signal characteristic of the complex is only observed at pH below 6, in agreement with the ^{13}C NMR experiments and quantification reported on Figure S3.

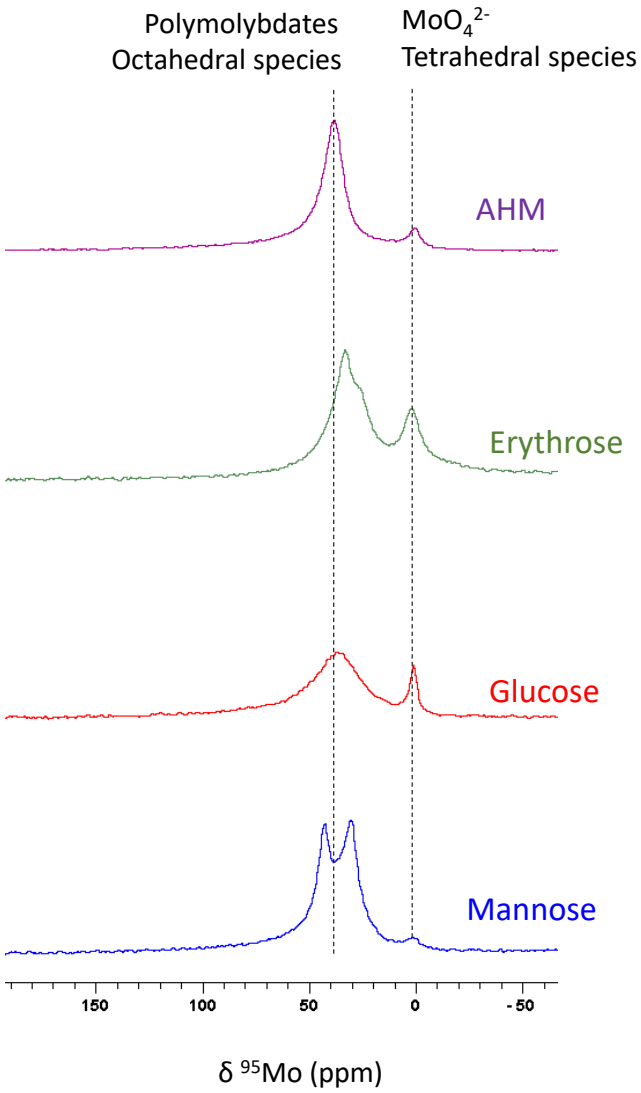

Figure 4. ^{95}Mo spectra recorded 1 hour after preparation at pH ≈ 6 of Na_2MoO_4 solutions with erythrose, glucose and mannose ([M] = 2 mol L^{-1}, [sugar] = 1 mol L^{-1}) compared to that of an aqueous ammonium heptamolybdate (AHM) solution of same metal ions concentration.

Figure 5a shows the W L_3-edge X-ray Absorption Spectroscopy in the near-edge region (XANES) of tungstate-sugars aqueous solutions, compared to the reference compounds ammonium metatungstate (AMT) and disodium tungstate (Na_2WO_4), prototypical compounds involving respectively octahedral and tetrahedral metallic centres. Glucose was not examined

herein as it does not form significant amounts of complexes detectable by NMR spectroscopy (Figure 2). The spectra recorded for mannose or erythrose with tungstate at pH 7 display the characteristic features of a W octahedral environment, namely by exhibiting a white line with a split top, with an energy gap between the two transitions of 3.3 and 3.5 eV, respectively (see second derivative plot on Figure S19) along with absence of the bump around 10224 eV (characteristic of W tetrahedral species).[25,26] However, these spectra remain significantly distinct from the spectrum of AMT (broader spectrum, splitting of 3.6 eV), showing the presence of different molecular structures. The edge energy referenced by the energy of the maximum of the first derivative is of 10210.3 and 10210.1 eV for mannose and erythrose-tungstate mixtures, respectively, which is fully in line with W^{6+} species, knowing that the edge energy of the fully oxidized Na_2WO_4 and AMT precursors ranges from 10209.9 to 10210.8 eV from our data. Figure 3b shows the Mo K-edge XANES spectra of molybdate-sugars solutions, together with the spectra of reference precursors ammonium heptamolybdate (AHM, octahedral species) and disodium molybdate (Na_2MoO_4, tetrahedral species). Here again, the spectra of sugar-molybdate mixtures at pH 6 are very similar to that of the reference AHM compound, with noticeably a weak pre-edge feature which is characteristic of the nearly centrosymmetric octahedral environment of molybdenum.[27,28] The edge energy is of 20015.0 and 20014.5 eV for molybdate-mannose and molybdate-erythrose mixtures, respectively, which falls in the typical range of Mo^{6+} species (20014.9 and 20016.4 eV for the precursors).[27,28]

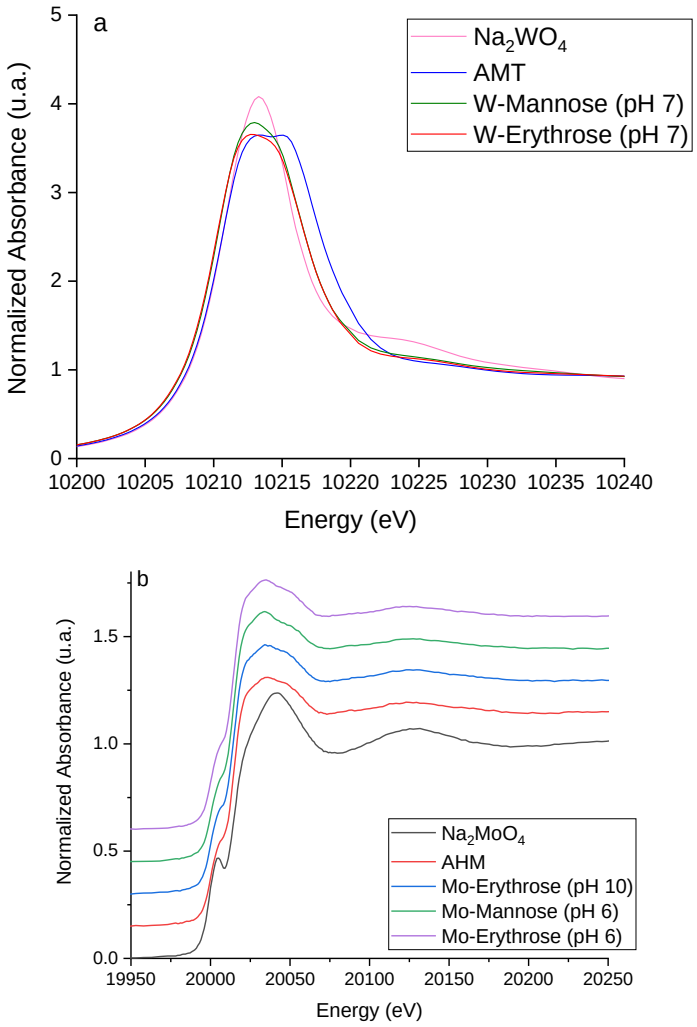

Figure 5. (a) W L_3-edge XANES normalized spectra of reference tungstate precursors and tungstate-sugars aqueous solutions, (b) Mo K-edge XANES normalized spectra of reference molybdate and molybdate-sugars aqueous solutions. [M] = 0.1 mol L^{-1}, [sugar] = 0.05 mol L^{-1}.

Thus far, our spectroscopic study shows that, with the exception of complex **D** formed by mannose and tungstate in basic medium already addressed in our previous study,[14] erythrose and mannose form with molybdate or tungstate in neutral aqueous solutions complexes with the metal in octahedral geometry in their oxidation state +VI. Besides, the analysis of the concentrations indicates that the nuclearity of these complexes is at most of 3.5 (mannose) or 2

(erythrose), *i.e.* significantly lower than that of the main inorganic species of the corresponding oxyanions in aqueous solution in such conditions ($W_{12}O_{40}^{8-}$ or $HMo_7O_{24}^{5-}$, see Figures S6-S7),[25,29] in line with earlier proposals with a nuclearity of two.[13,30,31] We constructed and optimized by means of DFT calculations a series of possible molecular models for each combination of metal and sugar under investigation, compelling to these latter observations. Similar models were proposed for glucose by analogy, although less data is available due to the low abundance of complexes. In order to assign a structure to each species, we adopted a similar procedure to that employed and detailed in our previous work for mannose-tungstate system,[14] namely (i) full characterization of the spectra of each species by combination of two dimensional ^{1}H-^{13}C heteronuclear and ^{1}H homonuclear NMR experiments (see Figures S8-13 and Table S1) (ii) calculation of the Coordination Induced Shift (CIS)[30] under the hypothesis of several tautomers (α and β pyranose and furanose, hydrate acyclic form) (iii) elimination of several possibilities based on geometric considerations depending on the tautomeric form (*e.g.* if some of the hydroxyl groups have an *anti*-configuration with respect to the cycle plan) (iv) structure optimization by DFT of the remaining possibilities and (v) comparison of the calculated chemical shift with the experimental values. Several types of complexes have been considered, including mononuclear and binuclear species, with several modes of denticity (Figure S20). The various data are provided in supporting information, along with the full reasoning for each complex (Tables S2-S6 for CIS analysis, Tables S7-S9 for theoretical vs. experimental values, Figures S21-S25 for the corresponding complex models). Note that we only report mono- and binuclear complexes, although higher nuclearity may be present. However, as we mentioned in our previous contribution,[14] every attempt to model a coordination to a higher oligomers involving more than two metal failed, only the models coordinating two M atoms succeeded, in

which case, as reported previously,[14] the NMR chemical shifts are similar to that calculated with a dinuclear complex with the same tautomer of the sugar and the same coordination sites. This shows that the dinuclear model is a suitable model for a coordination site of sugar on potentially higher metal oligomers. Energy data and procedure is documented in supporting information (Table S10).

Figure 6 shows the best matches in terms of ^{13}C chemical shifts for complexes **E**, **F**, **G**, **H** and **I** along with the corresponding structures. Complexes **A**, **B**, **C** and **D** were treated elsewhere[14] and not included on Figure 6a for the sake of clarity. The agreement between calculated and experimental value shows individual errors lower than 5 ppm and an average error of about 3 ppm for each complex (see Tables S2-S6, except G for which the error is 4 ppm due to a somewhat larger individual error of 9 ppm on C5).

According to the results of this multistep approach, complex **E** is a binuclear molybdate species coordinating β-mannofuranose at its O1,2,3,5 site with O2,5 bridging atoms (Figure 6, oxygen atoms are labelled according to the carbon atom bound to them); complex **F** features a binuclear molybdate site as well, bound to acyclic hydrated mannose form through its first four deprotonated hydroxyl groups (O1,2,3,4) in a "sickle" arrangement. Complexes **E** and **F** match with L and A type molybdate species of mannose previously described in the literature.[32] Species **G** involves a binuclear molybdate complex in which acyclic hydrated glucose is bound to the metallic center through a tetradentate O1,2,3,4 site in a "zigzag" arrangement with O2,3 as bridging oxygen atoms, analogous to the A type complex proposed in the literature for molybdate-glucose complexes.[32] Complex **H** and **I** formed by erythrose with tungstate and molybdate, respectively, are found to be isostructural. A dimeric metallic core is coordinated to the sugar through the first four vicinal deprotonated hydroxyl group O1,2,3,4 with O1,3 as

bridging atoms in a “sickle” arrangement. Note that the most abundant complexes determined with erythrose- and mannose-molybdate mixtures at pH 6 (Complexes I and E, respectively) are structurally different, which is consistent with the ^{95}Mo NMR showing quite different signals (see Figure 4).

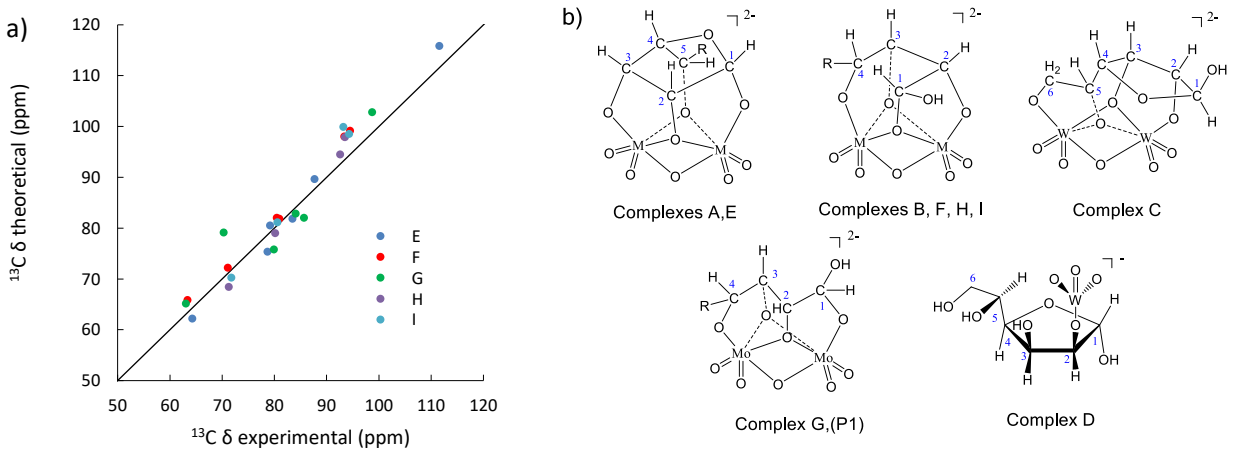

Figure 6. (a) Parity plot of experimental and DFT calculated ^{13}C NMR chemical shifts for the identified species E, F, G, H and I, the solid black line is the y = x plot as a guide to the eye; (b) Proposed structures for tungstate and molybdate complexes of C6 and C4 aldoses. M = W or Mo, R = CH_2OH or H, depending on the complex, see text and Figure 1.

As it can be seen, the series of complexes highlighted here feature a number of isostructural species, and in some cases similar species are formed as tungstate and molybdate complexes, namely the A/E, B/F and H/I couples. An interesting observation here is that in such case, the experimental chemical shift patterns are similar for the tungstate and molybdate version of the complex (Figure S26), which indicates that the deshielding of the carbon atoms by the coordination is independent of the nature of the metal. To go further, we plotted for all the optimized, theoretical complexes the ^{13}C chemical shifts for the molybdate version vs. that of the

tungstate version (Figure S27). We observe a very good correlation between the two sets of data, which confirms the general character of this observation. Hence, the CIS value is essentially a result of the structure adopted by the sugar, and the nature of the metal holds little influence on the chemical shielding. We use this property to tentatively assign a structure for complex P1, suggesting then a similar structure to that of complex **G** from the values of the chemical shifts of C1 and C3 measured thanks to the labelled glucose experiments, although more definitive assignment is not possible due to the incomplete spectrum obtained. However, no assignment could be made for **P2** despite thorough comparison to the calculated values.

Conclusion

Throughout this study, we could picture a detailed overview of the formation of complexes of several sugars of mechanistic interest in the production of ethylene glycol from biomass-based sugars (glucose, mannose and erythrose) with molybdate and tungstate oxyanions. Using a combination of spectroscopy (NMR and XANES) with DFT calculations, we distinguish a total of 10 identified species with very distinct speciation and pH dependence and could model a molecular structure for each of them, with calculated spectroscopic signatures matching the experimental one. We also highlight the intriguing behaviour of tungstate and molybdate oxyanions in catalyzing erythrose retro-aldol condensation in basic solution (pH around 10) at ambient temperature, and the formation of degradation products, which is of high catalytical importance as it reveals that tungstate and molybdate species of +VI oxidation state are active for this reaction, and also show the particularly high reactivity of erythrose, which might be a key parameter for the understanding of overall reactivity, and the detrimental formation of humins in particular. This opens door to the examination of the relationships between the speciation of such systems with their chemical reactivity.

ASSOCIATED CONTENT

Supporting Information. Additional 1D and 2D NMR spectra, Evolution with time of the quantification of the samples, additional XANES data, Speciation diagrams for molybdates and tungstates calculated by Medusa, Full data of calculated NMR spectra, Full depiction of the calculated structures, Full energetic data for the calculated complexes (.doc). Coordinates of the optimized species discussed in the manuscript are provided as Gaussian09 input (.com) and output files (.out) as well as in .xyz format.

The following files are available free of charge.

AUTHOR INFORMATION

Corresponding Author

Kim Larmier – IFP Energies nouvelles, Solaize 69360, France ; orcid.org/0000-0002-5199-1516 ; Email : kim.larmier@ifpen.fr

Notes

The authors declare no competing financial interests.

ACKNOWLEDGMENT

The authors acknowledge the European Synchrotron Radiation Facility (ESRF) (Grenoble, France) and the CRG-FAME BM30 beamline (French Absorption spectroscopy beamline in Material and Environmental science) staff for the XAS experiments. The authors kindly acknowledge David Proriol from IFPEN for his invaluable help in NMR measurements, especially ^{95}Mo NMR.

REFERENCES

(1) Wilson, K.; Lee, A. F. Bio-based chemicals from biorefining: carbohydrate conversion and utilisation. In *Advances in Biorefineries*; Elsevier, 2014; pp 624–658. DOI: 10.1533/9780857097385.2.624.

(2) Naqvi, S. N.; Chang, R. J. *Ethylene Glycol Production from Coal-Based Synthesis Gas*.

(3) Zheng, M.; Pang, J.; Sun, R.; Wang, A.; Zhang, T. Selectivity Control for Cellulose to Diols: Dancing on Eggs. *ACS Catal.* **2017**, *7* (3), 1939–1954. DOI: 10.1021/acscatal.6b03469.

(4) Zhang, J.; Liu, X.; Sun, M.; Ma, X.; Han, Y. Direct Conversion of Cellulose to Glycolic Acid with a Phosphomolybdic Acid Catalyst in a Water Medium. *ACS Catal.* **2012**, *2* (8), 1698–1702. DOI: 10.1021/cs300342k.

(5) Zhang, J.; Hou, B.; Wang, A.; Li, Z.; Wang, H.; Zhang, T. Kinetic study of the competitive hydrogenation of glycolaldehyde and glucose on Ru/C with or without AMT. *AIChE J.* **2015**, *61* (1), 224–238. DOI: 10.1002/aic.14639.

(6) Zhou, J.; Liu, G.; Sui, Z.; Zhou, X.; Yuan, W. Hydrogenolysis of sorbitol to glycols over carbon nanofibers-supported ruthenium catalyst:The role of base promoter. *Chinese Journal of Catalysis* **2014**, *35* (5), 692–702. DOI: 10.1016/S1872-2067(14)60083-8.

(7) Wang, A.; Zhang, T. One-pot conversion of cellulose to ethylene glycol with multifunctional tungsten-based catalysts. *Accounts of chemical research* **2013**, *46* (7), 1377–1386. DOI: 10.1021/ar3002156.

(8) Liu, Y.; Zhang, W.; Hao, C.; Wang, S.; Liu, H. Unveiling the mechanism for selective cleavage of C-C bonds in sugar reactions on tungsten trioxide-based catalysts. *Proceedings of the National Academy of Sciences of the United States of America* **2022**, *119* (34), e2206399119. DOI: 10.1073/pnas.2206399119. Published Online: Aug. 19, 2022.

(9) Chapelle, S.; Sauvage, J.-P.; Verchère, J.-F. 183W NMR Studies of Tungstate Complexes of Carbohydrates. 2. Competitive Formation of erythro and threo Complexes of Alditols. Characterization of a Novel Bis-Dinuclear Complex Formed with Perseitol. *Inorganic Chemistry* **1994**, *33*, 1966–1971.

(10) Chapelle, S.; Verchère, J.-F. A carbon-13 NMR study of the tungstate and molybdate complexes of perseitol, galacticol and mannitol. *Carbohydrate research* **1991**, *211*, 279–286.

(11) Chapelle, S.; Verchère, J.-F. Tungsten-183 NMR studies of tungstate complexes of carbohydrates. 1. Characterization of two structural types in the alditol series. Evidence that the tungstate and molybdate threo complexes are not homologous. *Inorganic Chemistry* **1992**, *31*, 648–652.

(12) Matulova, M.; Verchère, J.-F.; Chapelle, S. Furanose vs. acyclic forms of carbohydrate ligands. A multinuclear NMR spectroscopy of the molybdate and tungstate complexes of D-glycero-L-manno-heptose. *Carbohydrate research* **1996**, *287*, 37–48.

(13) Bilik, V.; Matulova, M. Reactions of saccharides catalyzed by molybdate ions XLII. Epimerization and the molybdate complexes of aldoses. *Chemical Papers* **1990**, *44*, 257–265.

(14) El Mohammad, S.; Proux, O.; Aguilar, A.; Hazemann, J. L.; Legens, C.; Chizallet, C.; Larmier, K. Elucidation of Metal-Sugar Complexes: When Tungstate Combines with D-Mannose. *Inorganic Chemistry* **2023**, *62*, 7545–7556.

(15) Proux, O.; Nassif, V.; Prat, A.; Ulrich, O.; Lahera, E.; Biquard, X.; Menthonnex, J. J.; Hazemann, J. L. Feedback system of a liquid-nitrogen-cooled double-crystal monochromator: design and performances. *Journal of synchrotron radiation* **2006**, *13* (Pt 1), 59–68. DOI: 10.1107/S0909049505037441. Published Online: Dec. 22, 2005.

(16) Proux, O.; Biquard, X.; Lahera, E.; Menthonnex, J.-J.; Prat, A.; Ulrich, O.; Soldo, Y.; Trévisson, P.; Kapoujyan, G.; Perroux, G.; Taunier, P.; Grand, D.; Jeantet, P.; Deleglise, M.; Roux, J.-P.; Hazemann, J. L. FAME: a New Beamline for X-Ray Absorption Investigations of Very-Diluted Systems of Environmental, Material and Biological Interests. *Physica Scripta* **2005**, *T115*, 970–973.

(17) Frisch, M. J.; Trucks, G. W.; Schlegel, H. B.; Scuseria, G. E.; Robb, M. A.; Cheeseman, J. R.; Scalmani, G.; Barone, V.; Petersson, G. A.; Nakatsuji, H.; Li, X.; Caricato, M.; Marenich, A.; Bloino, J.; Janesko, B. G.; Gomperts, R.; Mennucci, B.; Hratchain, H. P.; Ortiz, J. V.; Izmaylov, A. F.; Sonnenberg, J. L.; Williams-Young, D.; Ding, F.; Lipparini, F.; Egidi, F.; Goings, J.; Peng, B.; Petrone, A.; Henderson, T.; Ranasinghe, D.; Zakrzewski, V. G.; Gao, J.; Rega, N.; Zheng, G.; Liang, W.; Hada, M.; Ehara, M.; Toyota, K.; Fukuda, R.; Hasegawa, J.; Ishida, M.; Nakajima, T.; Honda, Y.; Kitao, O.; Nakai, H.; Vreven, T.; Throssell, K.; Montgomery, J. A.; Peralta, J. E.; Ogliaro, F.; Bearpark, M.; Heyd, J. J.; Brothers, E.; Kudin, K. N.; Staroverov, V. N.; Keith, T.; Kobayashi, R.; Normand, J.; Raghavachari, K.; Rendell, A.; Burant, J. C.; Iyengar, S. S.; Tomasi, J.; Cossi, M.; Millam, J. M.; Klene, M.; Adamo, C.; Cammi, R.; Ochterski, J. W.; Martin, R. L.; Morokuma, K.; Farkas, O.; Foresman, J. B.; Fox, D. J. *Gaussian 09, Revision B.01*; Gaussian, Inc., Wallingford CT, 2010.

(18) Becke, A. D. Density-functional thermochemistry. III. The role of exact exchange. *The Journal of Chemical Physics* **1993**, *98*, 5648–5652.

(19) Lee, C.; Yang, W.; Parr, R. G. Decelopment of the Colle-Salvetti Correlation-Energy Formula into a Functional of the Electron Density. *Physical Review B* **1988**, *37* (2).

(20) Miehlich, B.; Savin, A.; Stoll, H.; Preuss, H. Results Obtained with the Correlation Energy Density Functionals of Becke and Lee, Yang and Parr. *Chemical Physics Letters* **1989**, *157* (3), 200–206.

(21) Weigend, F.; Ahlrichs, R. Balanced basis sets of split valence, triple zeta valence and quadruple zeta valence quality for H to Rn: Design and assessment of accuracy. *Physical chemistry chemical physics : PCCP* **2005**, *7* (18), 3297–3305. DOI: 10.1039/b508541a. Published Online: Aug. 4, 2005.

(22) Weigend, F. Accurate Coulomb-fitting basis sets for H to Rn. *Physical chemistry chemical physics : PCCP* **2006**, *8* (9), 1057–1065. DOI: 10.1039/b515623h. Published Online: Jan. 3, 2006.

(23) Pritchard, B. P.; Altarawy, D.; Didier, B.; Gibson, T. D.; Windus, T. L. New Basis Set Exchange: An Open, Up-to-Date Resource for the Molecular Sciences Community. *Journal of chemical information and modeling* **2019**, *59* (11), 4814–4820. DOI: 10.1021/acs.jcim.9b00725. Published Online: Oct. 24, 2019.

(24) Malito, J. Molybdenum-95 NMR Spectroscopy. *Annual Reports on NMR Spectroscopy* **1996**, *33*, 151–206.

(25) Hur, H.; Reeder, R. J. Tungstate sorption mechanisms on boehmite: Systematic uptake studies and X-ray absorption spectroscopy analysis. *Journal of colloid and interface science* **2016**, *461*, 249–260. DOI: 10.1016/j.jcis.2015.09.011. Published Online: Sep. 5, 2015.

(26) Yamazoe, S.; Hitomi, Y.; Shishido, T.; Tanaka, T. XAFS Study of Tungsten L1- and L3-Edges: Structural Analysis of WO3 Species Loaded on TiO2 as a Catalyst for Photo-oxidation of NH3. *J. Phys. Chem. C* **2008**, *112* (17), 6869–6879. DOI: 10.1021/jp711250f.

(27) Tougerti, A.; Berrier, E.; Mamede, A.-S.; La Fontaine, C.; Briois, V.; Joly, Y.; Payen, E.; Paul, J.-F.; Cristol, S. Synergy between XANES Spectroscopy and DFT to Elucidate the Amorphous Structure of Heterogeneous Catalysts: TiO 2 -Supported Molybdenum Oxide Catalysts. *Angew. Chem.* **2013**, *125* (25), 6568–6572. DOI: 10.1002/ange.201300538.

(28) Rochet, A.; Baubet, B.; Moizan, V.; Pichon, C.; Briois, V. Co-K and Mo-K edges Quick-XAS study of the sulphidation properties of Mo/Al2O3 and CoMo/Al2O3 catalysts. *Comptes Rendus Chimie* **2016**, *19* (10), 1337–1351. DOI: 10.1016/j.crci.2016.01.009.

(29) Oyerinde, O. F.; Weeks, C. L.; Anbar, A. D.; Spiro, T. G. Solution structure of molybdic acid from Raman spectroscopy and DFT analysis. *Inorganica Chimica Acta* **2008**, *361* (4), 1000–1007. DOI: 10.1016/j.ica.2007.06.025.

(30) Verchère, J.-F.; Sauvage, J.-P.; Rapaumbya, G.-R. Comparative study of various polyols as complexing agents for the acidimetric titration of tungstate. *Analyst* **1990**, *115*, 637–640.

(31) Chethana, B. K.; Lee, D.; Mushrif, S. H. First principles investigation into the metal catalysed 1,2 carbon shift reaction for the epimerization of sugars. *Journal of Molecular Catalysis A: Chemical* **2015**, *410*, 66–73. DOI: 10.1016/j.molcata.2015.09.004.

(32) Chapelle, S.; Verchère, J.-F. Tungstate complexes of aldoses and ketoses of the lyxo series. Multinuclear NMR evidence for chelation by one or two oxygen atoms borne by the side chain of the furanose ring. *Carbohydrate research* **1995**, *277*, 39–50.

For Table of Contents Only

TOC Graphics

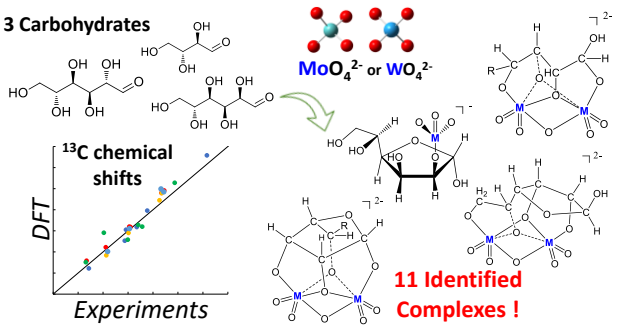

Synopsis

The aqueous speciation of tungstates and molybdates oxoanions with glucose, mannose erythrose is examined by combined NMR spectroscopy, XAS spectroscopy and DFT. Eleven complexes are identified depending on the metal, sugar and pH conditions, with very good agreement between experimental and calculated ^{13}C chemical shifts.